Microstructural and mechanical properties of Ti₃SiC₂-CNF composite materials by PM

TM ile üretilen Ti₃SiC₂-KNF kompozit malzemelerin mikroyapı ve mekanik özellikleri

Yazar(lar) (Author(s)): Abdualkarim Musbah M. GARİBA[1], Faik OKAY[2], Ibtesam Said Shneeb SAİD[3], Serkan ISLAK[4]

ORCID[1]: 0000-0001-7031-509X

ORCID[2]: 0000-0001-5072-7492

ORCID[3]: 0000-0001-7593-8560

ORCID[4]: 0000-0001-9140-6476

Microstructural and Mechanical Properties of Ti$_3$SiC$_2$-CNF Composite Materials by PM

Highlights

❖ *MAX phase composite material was successfully manufactured*

❖ *Intensity of MAX phase increased even more with increasing sintering temperature.*

❖ *With the increase of sintering temperature, binary and ternary complex phases were formed.*

Graphical Abstract

The powders mixing process was carried out by a ball milling apparatus. The cold pressing process was carried out using a hydraulic press. Sintering process was carried out at argon atmosphere at 1150 °C, 1300 °C and 1450 °C for 2 h.
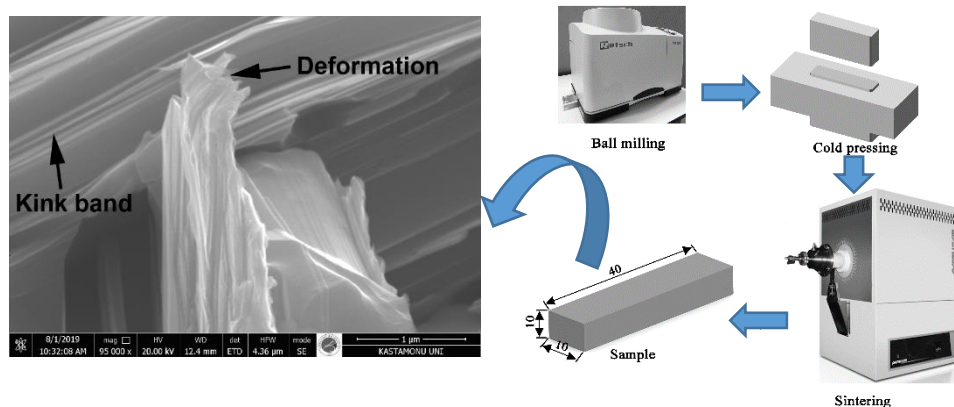
Figure. Production schematic of samples

Aim

This study aims to investigate the microstructure and mechanical properties of Ti$_3$SiC$_2$-carbon nanofiber (CNF) composite materials by powder metallurgy (PM). Ti, SiC, graphite and CNF powders were used to produce Ti$_3$SiC$_2$-CNF composite materials.

Design & Methodology

The Ti$_3$SiC$_2$-CNF composite material was manufactured from four different powders using powder metallurgy (PM). Sintering process was carried out at argon atmosphere at 1150 °C, 1300 °C and 1450 °C.

Originality

The study on MAX phase composite materials is very limited. In this study, microstructure, density, hardness and mechanical characteristics of Ti$_3$SiC$_2$-CNF composite materials produced by powder metallurgy were investigated.

Findings

With the increase of sintering temperature, both the experimental and relative densities of the samples have increased significantly. Microhardness values have changed considerably with increasing sintering temperature. As the sintering temperature increased, the TRS values of the samples increased.

Conclusion

MAX phase matrix CNF reinforced materials with kink band structure have been successfully produced. With the increase of sintering temperature, these structures have become more evident.

Declaration of Ethical Standards

The author(s) of this article declare that the materials and methods used in this study do not require ethical committee permission and/or legal-special permission.

TM ile Üretilen Ti₃SiC₂-KNF Kompozit Malzemelerin Mikroyapı ve Mekanik Özellikleri

Araştırma Makalesi / Research Article

Abdualkarim Musbah M. GARİBA[1], Faik OKAY[2], Ibtesam Said Shneeb SAİD[1], Serkan ISLAK[3*]

[1]Fen Bilimleri Enstitüsü, Malzeme Bilimi ve Mühendisliği Anabilim Dalı, Kastamonu Üniversitesi, Türkiye
[2]Kastamonu Meslek Yüksek Okulu, Makine Bölümü, Kastamonu Üniversitesi, Türkiye
[3]Mühendislik ve Mimarlık Fakültesi, Makine Mühendisliği Bölümü, Kastamonu Üniversitesi, Türkiye

ÖZ

Bu çalışma, toz metalurjisi (TM) ile üretilen Ti₃SiC₂-karbon nanofiber (KNF) kompozit malzemelerin mikroyapısı ve mekanik özelliklerini araştırmayı amaçlamaktadır. Ti, SiC, grafit ve KNF tozları Ti₃SiC₂-KNF kompozit malzemeleri üretmek için kullanılmıştır. Formülize edilen tozlar mekanik alaşımlandıktan sonra, 500 MPa'da preslenip 1150 °C, 1300 °C ve 1450 °C'de sinterlenmiştir. Mikroyapı ve faz oluşumunu incelemek için SEM-EDS ve XRD analizleri kullanılmıştır. Sertlik testi Vickers sertlik test cihazı yardımıyla gerçekleştirilmiştir. Yoğunluklar Arşimet prensibi ile ölçülmüştür. Numunelerin çapraz kırılma dayanımlarını (ÇKD) belirlemek için üç noktalı eğilme testi yapılmıştır. SEM görüntüleri, numunelerin MAX faz materyallerine özgü kink bandı ve nanolaminar yapılara sahip olduğunu göstermiştir. XRD analizi ile tespit edilen Ti₃SiC₂ fazının varlığı da bu durumu desteklemektedir. Sinterleme sıcaklığına bağlı olarak, numunelerin mikroyapısı, yoğunluğu ve mekanik özelliklerinde değişiklikler olmuştur.

Anahtar Kelimeler: Ti₃SiC₂, KNF, MAX fazı, mikroyapı, sertlik, ÇKD.

Microstructural and Mechanical Properties of Ti₃SiC₂-CNF Composite Materials by PM

ABSTRACT

This study aims to investigate the microstructure and mechanical properties of Ti₃SiC₂-carbon nanofiber (CNF) composite materials by powder metallurgy (PM). Ti, SiC, graphite and CNF powders were used to produce Ti₃SiC₂-CNF composite materials. After formulated powders were ground in a ball mill, the milled powders were pressed at 500 MPa pressure and then sintered at 1150 °C, 1300 °C and 1450 °C. SEM-EDS and XRD analysis were used to examine the microstructure and phase formation. Hardness test was carried out with the help of Vickers hardness test apparatus. The densities were measured by Archimedes' principle. Three-point bending test was performed to determine the transverse rupture strength (TRS) of the samples. SEM images showed that the samples have kink band and nanolaminar structures typical of MAX phase materials. The presence of Ti₃SiC₂ phase detected by XRD analysis also supports this situation. Depending on the sintering temperature, there were changes in the microstructure, density and mechanical properties of the samples.

Keywords: Ti₃SiC₂, CNF, MAX phase, microstructure, hardness, TRS.

1. INTRODUCTION

Metallic materials are characterized by good thermal and electrical conductivity, plastic deformable, easily machinable, good thermal shock resistance, and partly by softness. On the other hand, ceramic materials are characterized by high elasticity modulus and corrosion resistance and excellent stable mechanical features at high temperatures. Recently, new materials have been found in the name of MAX phase which has the properties of both metallic materials and ceramic materials as a result of intensive work on advanced materials [1,2].

The term $M_{n+1}AX_n$ phase was first used by Michel W. Barsoum in 2000. Then, in the general formula $M_{n+1}AX_n$ of the abbreviated phases, n=1-3, M=transition metal, A=generally the IIIA and IVA group elements, and finally X represents carbon (C) or nitrogen (N). Figure 1 shows the formation of MAX phases in the periodic table. The transition metals in the ruler are Sc, Mo, Ti, Ta, V, Hf, Nb, Cr and Zr. Depending on the value of n, the MAX phases in the form of M_2AX, M_3AX_2 and M_4AX_3 are represented as 211, 312, and 413, respectively [3]. In the literature, 514, 615 and 716 MAX phases have been reported in the order [4,5].

MAX phase materials have a different application area. Figure 2 shows the application of several MAX phases. MAX phases are still in the testing phase in most of these areas of application. The physical properties of about 240 MAX phases, which are both experimentally and theoretically examined, are not fully understood [6-10]. In the studies conducted with MAX phases, cold pressing (CP)+sintering, hot pressing (HP), hot isostatic pressing (HIP), chemical vapor deposition (CVD), self-advancing high temperature synthesis (SHS), thermal spraying, mechanical alloying, magnetron sputtering and

Sorumlu Yazar (Corresponding Author)
e-posta : serkan@kastamonu.edu.tr

combustion reaction methods. The MAX phases were obtained in the form of powder, bulk material or thin film coating [11].
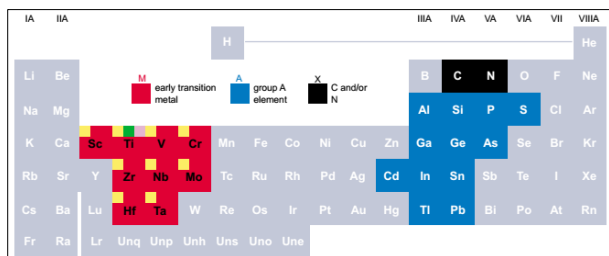
Fig. 1. Formation of MAX phases in periodic table.
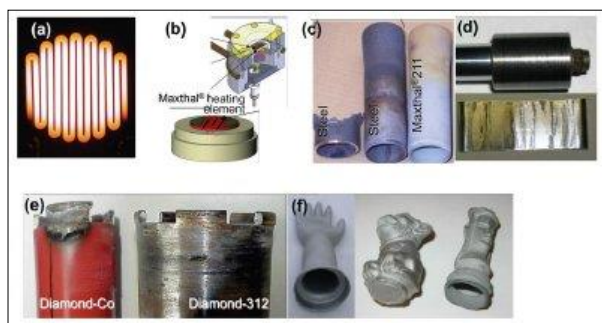
Fig. 2. MAX phase applications; (a) and (b) heating elements, (c) burner nozzle, (d) high temperature bearings, (e) diamond/Ti₃SiC₂ composite drills and (f) slip-cast thin-walled casting products [12].

In the literature, studies on Ti_3SiC_2 [13-15], Ti_3AlC_2 [15, 16], Ti_2AlC [17], Cr_2AlC [18, 19], V_2AlC [20], Nb_4AlC_3 [21] and Nb_2SiC [22] MAX phase materials are generally available. The properties of these materials such as oxidation, fracture, microstructure, phase analysis and abrasion are investigated in detail. Furthermore, Ti_2AlC and Ti_3SiC_2 phase materials are patented as heating elements under the name MAXthal 211 and MAXthal 312. These materials have been reported to have superior properties than titanium. However, the study on MAX phase composite materials is very limited. In this study, microstructure, density, hardness and mechanical characteristics of Ti_3SiC_2-CNF composite materials produced by powder metallurgy were investigated.

2. MATERIAL AND METHOD

The Ti_3SiC_2-CNF composite material was manufactured from four different powders using powder metallurgy (PM). The mixtures were Ti, SiC, graphite and CNF. The reactant powders were obtained from titanium powder (Sigma–Aldrich, particle size -325 mesh, purity 99.5%), silicon carbide powder (Sigma–Aldrich, -325 mesh, purity 99%), graphite powder (Sigma–Aldrich, <2 μm, 99.5%) and carbon nanofiber powder (Sigma–Aldrich, graphitized, >98% carbon basis, D×L 100 nm×20-200 μm). SEM photographs of the powders are shown in Figure 3. Ti, graphite and SiC powders have complex morphology, while CNF fiber has morphology. Ti + 25% SiC + 4.5% C and 0.5% CNF powder mixture was used to obtain the Ti_3SiC_2-CNF composite. The powders

mixing process was carried out by a ball milling apparatus (Model PM 100, Retsch Co. Germany) in a container with ten stainless steel balls of 10 mm diameter. The weight ratio of the ball to the powder is set to 10:1. The speed of the container was selected as 450 rpm. Ball milling time was 2 h. The prepared powders were placed in the cold pressing mold. The cold pressing process was carried out using a Specac hydraulic press by applying a pressure of 500 MPa. Sintering process was carried out at argon atmosphere at 1150 °C, 1300 °C and 1450 °C for 2 h. Samples were produced in 40 mm x 10 mm x 10 mm for both microstructural examination and three-point bending test. The production schematic of the samples is given in Figure 4.
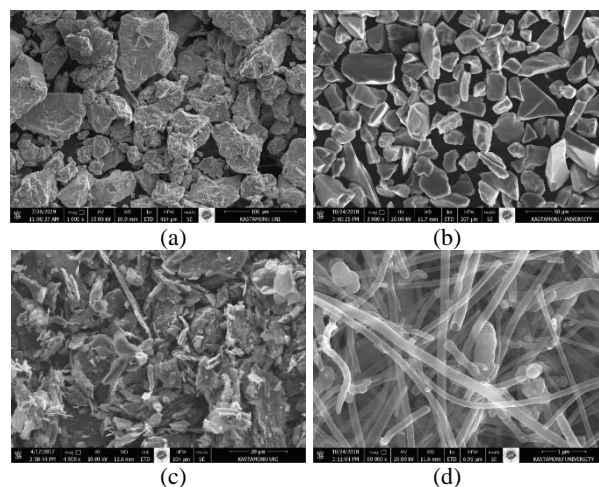
Fig. 3. SEM images of powders: (a) Ti, (b) SiC, (c) graphite and (d) CNF
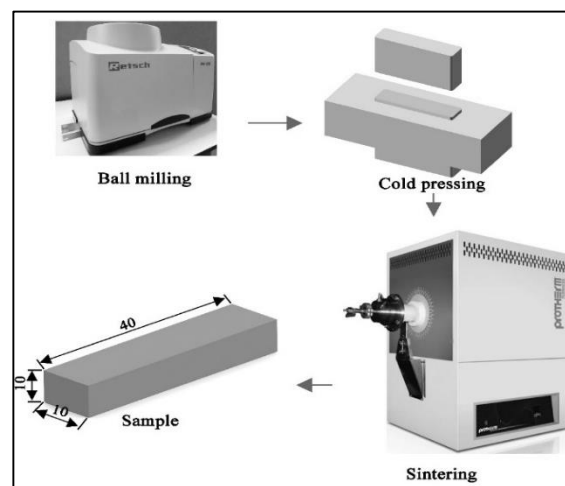
Fig. 4. Production schematic of samples

SEM, XRD, microhardness, density and transverse rupture strength (TRS) were performed for the samples. The SEM-EDS analyzes of the samples were obtained from the FEI brand Quanta FEG 250 model device. The XRD analyzes of the samples were taken from Bruker brand D8 Advance model device. The hardness measurements of the materials were done by using Shimadzu brand HMV-G21 model microhardness

measurement device under 15 second waiting time and 200 g load. The densities were calculated by using the Archimedes' principle. Three-point bending tests to determine the TRS were performed in accordance with the ASTM B 528-83a standard using a Shimadzu AG-X Universal Test Machine with 50 kN load capacity.

3. RESULTS AND DISCUSSIONS

SEM photograph and XRD pattern of the alloyed powder produced after ball milling process are given in Figure 5.

After the ball milling process, it is seen from Figure 5a that the powders have different morphology, such as spherical, angular and sticky. As a result of the milling process, the raw powders had a completely different morphology. CNF is clearly visible in the powder grain in zone A (Fig. 5b). In the XRD pattern given in Figure 5c, the phases formed in the synthesized powder were detected. Ti, TiC, SiC, C, Ti$_3$SiC$_2$ phases were formed in microstructure. TiC and Ti$_3$SiC$_2$ are newly formed phases. The presence of the Ti$_3$SiC$_2$ phase indicates that the MAX phase is obtained in the powder.
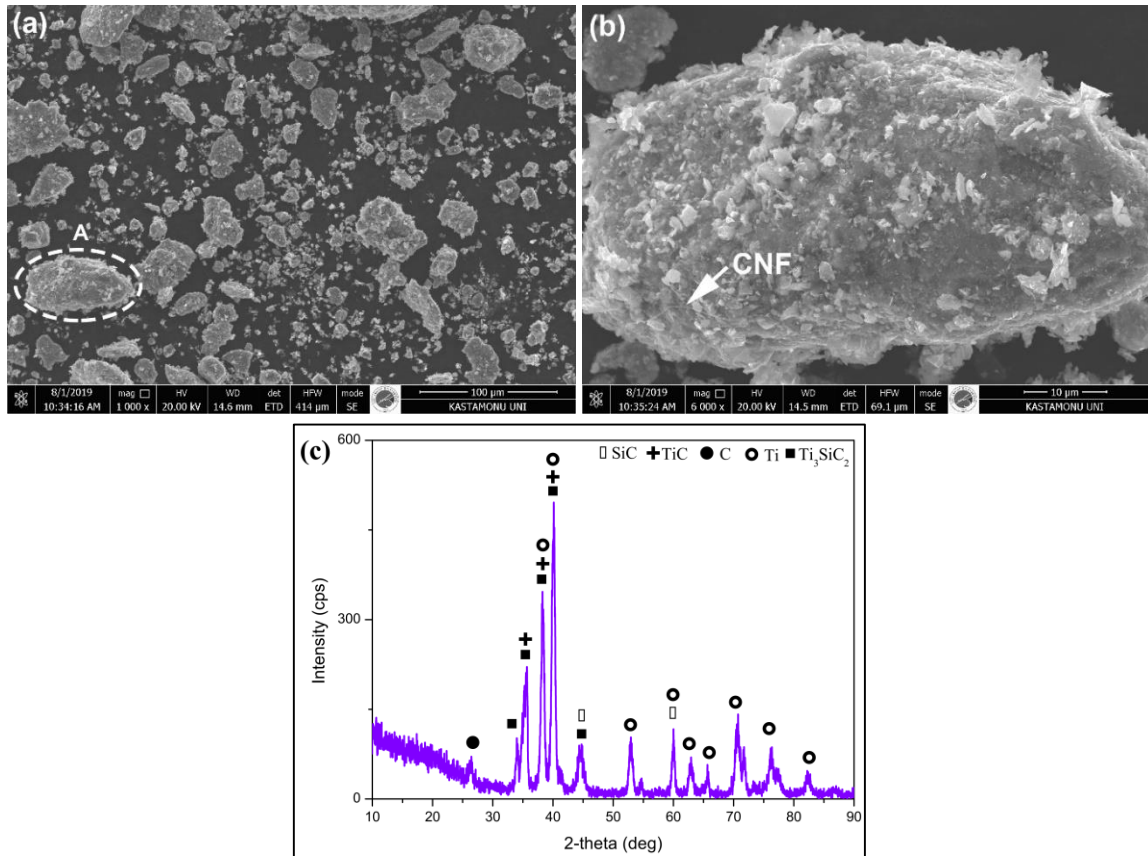
Fig. 5. (a, b) SEM images at different magnifications and (c) XRD pattern of ball milled powder

The XRD patterns of cold pressed and then sintered samples at 1150 °C, 1300 °C and 1450 °C are shown in Figure 6. Similar phases were determined at all three temperatures, SiC, TiC, C, Ti$_3$SiC$_2$, Ti$_5$Si$_3$ and TiSi$_2$. The peaks of these phases can be easily identified in Figure 6. XRD patterns also show that all Ti in the starting powder reacts to form different phases. With increasing sintering temperature, the intensity of the peaks of TiC, Ti$_3$SiC$_2$, Ti$_5$Si$_3$ and TiSi$_2$ phases increased. This can be related to the increase in reactivity with temperature increase [23-25]. Unlike milled but not sintered powder, Ti$_5$Si$_3$ and TiSi2 phases were formed in sintered samples. In addition, Ti is completely lost. This is highlighted above. In addition, the graph shows the decrease in the peaks of the SiC phase. This can be explained by the degradation of SiC at high temperatures. Degradation products combine with Ti to form other binary (TiC, Ti$_5$Si$_3$ and TiSi$_2$) and triple phases (Ti$_3$SiC$_2$) [26].
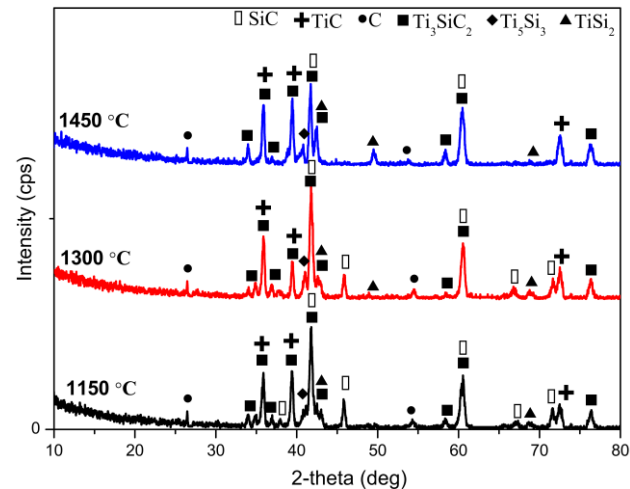
Fig. 6. XRD pattern of sintered samples

SEM photographs of samples sintered at 1150 °C, 1300 °C and 1450 °C and EDS analysis of some regions are shown in Figure 7-Figure 9 in detail. Figure 7 shows that the sample is partially porous from the photograph of the sintered sample at 1150 °C. In the same photo, CNFs are clearly visible.
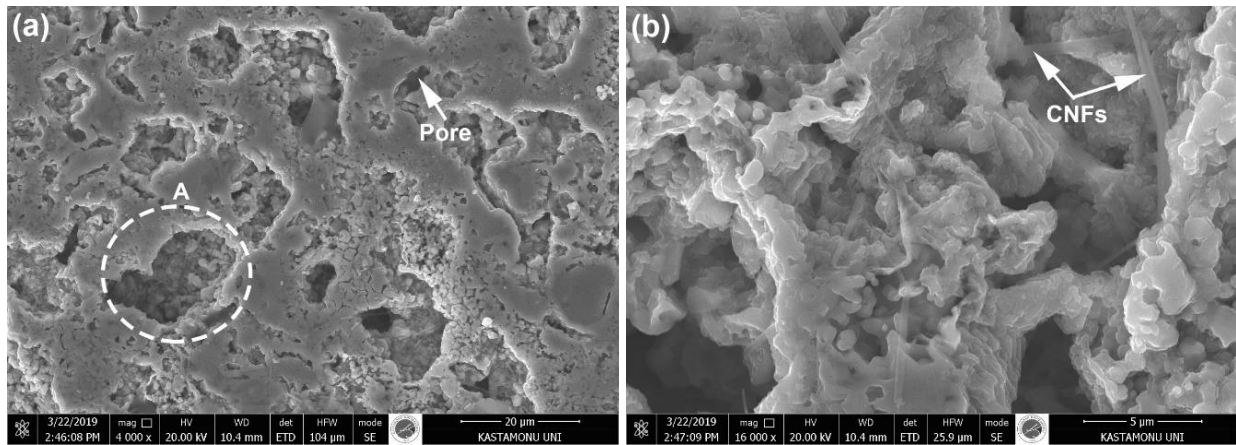
Fig. 7. (a) SEM image of sample sintered at 1150 °C and (b) an enlarged view of area A

The microstructure changes are remarkable when the sintering temperature increases from 1150 °C to 1300 °C (Figure 8). Particularly remarkable structures are rod structures. These rod structures are thought to be Ti_5Si_3 phase structures considering EDS analysis and morphology. Ding et al. (2019) in their study on Ti-C-Si systems and formation mechanisms, they identified the structure with Ti_5Si_3 rod [27]. Reported the formation of this structure according to $Ti+Si \rightarrow Ti_5Si_3$ reaction. In our study, EDS analysis of this phase is given in Figure 8b.

The composition of the phase is 62.4% Ti and 37.6% Si by weight. Again, Figure 8 shows the presence of TiC and $TiSi_2$ phase structures. The reaction of high amount of Si with Ti at high temperature resulted in $TiSi_2$ phase. The EDS analysis of this phase is 46.5% Ti and 53.5% Si. These phases are also seen in the Ti-Si-C triple phase diagram in Figure 10. In the diagram, the formation of the $TiSi_2$ phase is supported as the Si corner goes.
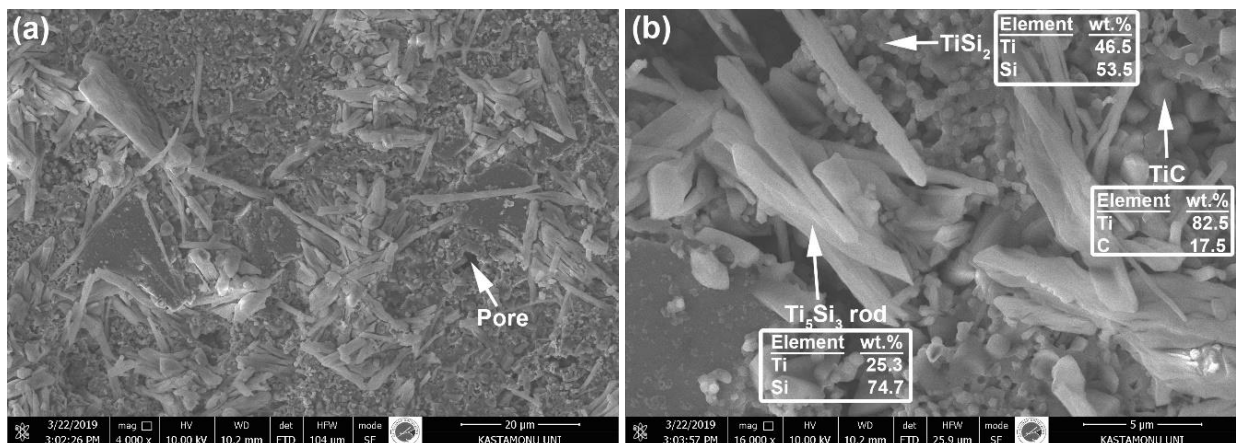
Fig. 8. (a) SEM image of sample sintered at 1300 °C and (b) an enlarged view and EDS analysis

When the sintering temperature reaches 1450 °C, the structure and phases of carbon nanofiber, TiC and Ti_3SiC_2 are seen in the microstructure (Figure 9). It is understood from the microstructure that the Ti_5Si_3 rod structure disappeared with increasing TiC amount. The formation of TiC network can be explained as inhibiting the formation of Ti_5Si_3 phase [27]. For the sample sintered at 1450 °C, the Ti_3SiC_2 phase is evident in the microstructure of the polished and etched sample. The EDS analysis of this phase was 47.9% Ti, 17.2% Si and 34.9% C by weight. The Ti_3SiC_2 phase is seen as the T1 phase in the Ti-Si-C ternary phase diagram. The chemical composition is close to the values in the phase diagram. TiC react with Ti-Si and if carbon is present in the environment, the Ti_3SiC_2 phase is nucleated from TiC and transforms into a layered structure [28].

190
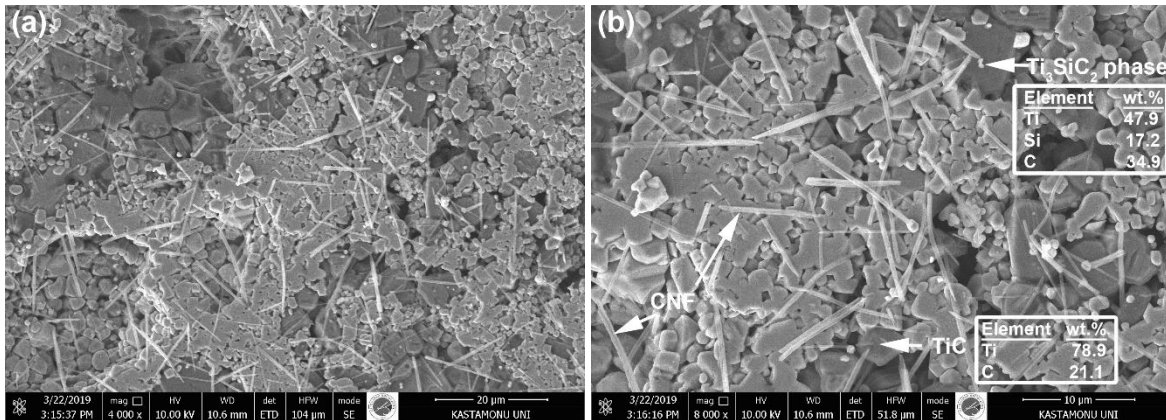
Fig. 9. (a) SEM image of sample sintered at 1450 °C and (b) an enlarged view and EDS analysis
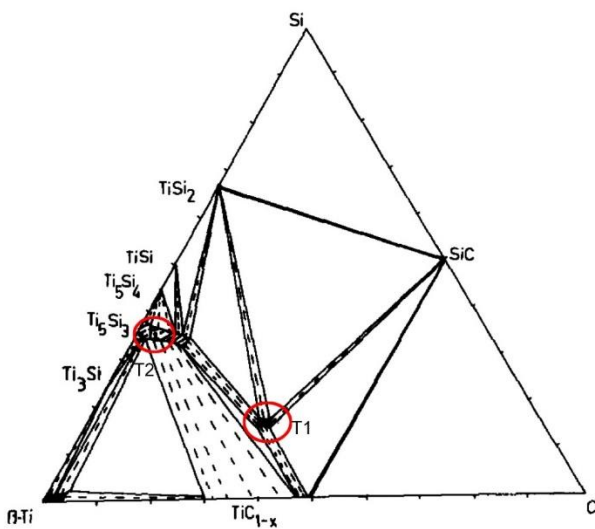
Fig. 10. Ti-Si-C phase diagram at 1373 K temperature [29].

Table 1 shows the experimental and relative densities of Ti₃SiC₂-CNF materials. Experimental densities range from 3.4294 to 3.7542 g/cm³. Relative densities range from 84.39% to 92.38%. By increasing the sintering temperature, both experimental and relative densities were significantly increased. At higher sintering temperatures, a denser structure was formed due to higher diffusion rates [30-32].

Table 1. Densities of samples

Sintering temperature (°C)	Experimental density (g/cm³)	Relative density (%)
1150	3,4294	84,39
1300	3,5159	86,52
1450	3,7542	92,38

The graph of hardness of Ti₃SiC₂-CNF materials is given in Figure 11. Microhardness values ranged from 255 HV₀.₂ to 278 HV₀.₂ with increasing sintering temperature. The hardness of the samples is 255 HV₀.₂, 278 HV₀.₂ and 268 HV₀.₂ for samples sintered at 1150 °C, 1300 °C and 1450 °C, respectively. Hardness increased while the sintering temperature increased from 1150 °C to 1300 °C,

and the hardness partially decreased as the temperature increased from 1300 °C to 1450 °C. The presence of partial pores at 1100 °C caused the hardness to be slightly lower. The high microhardness at 1300 °C is mainly due to the presence of hard phases such as TiC and Ti₅Si₃. The decrease in hardness at 1450 °C is the presence of increased Ti₃SiC₂ phase. Liu et al. (2009) is based on the presence of soft and monolithic Ti₃SiC₂ [33]. Magnus et al. (2020) explained this situation with the scarcity of hard phases in the structure such as TiC and TiSi₂ [34].
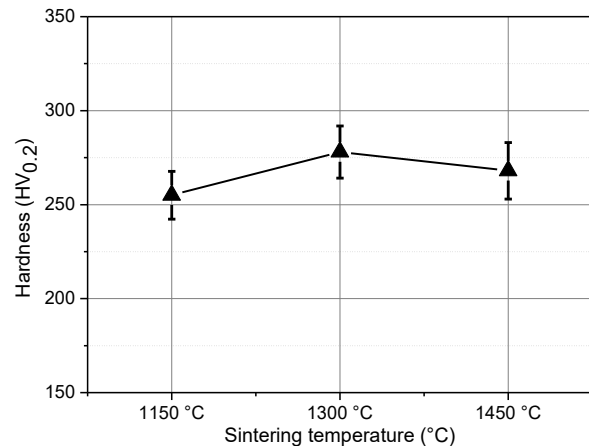
Fig. 11. Graph of hardness of Ti₃SiC₂-CNF materials

The effect of sintering temperature on TRS can be seen in Figure 12. If the sintering temperature increases, the TRS of the samples increased. However, similar TRS value has been determined for 1300 °C and 1450 °C sintering temperatures. The TRS values at 1150, 1300 and 1450 °C for the samples are 445 MPa, 490 MPa and 485 MPa, respectively. The reason of the low strength in the first sample (1150 °C) is that the pores present in the structure create a notch effect and create a weakening effect. With the effect of temperature, the pores are closed due to solid-state diffusion and therefore an increase in strength has occurred [35, 36]. However, the fact that the resistance at 1450 °C decreases very little is the presence of soft ceramic phase (Ti₃SiC₂) in the microstructure.
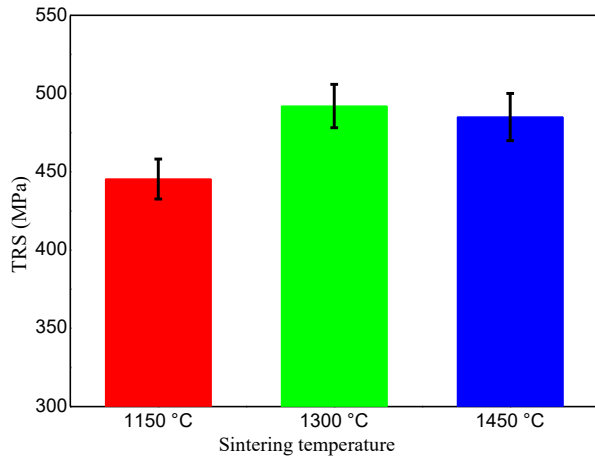
Fig. 12. TRS graph of samples

condition of the fracture surfaces. SEM examinations of the surfaces of the samples are given in Figure 13- Figure 15. It is seen that the fracture pattern in all three samples is not brittle. Toughness phenomena in these samples are crack propagation through the fibers in different directions, separation of the fiber and pulling out of the fiber. The inclusion of the MAX phase in composites not only strengthens the hardening mechanism of the matrix, but the matrix itself has also an important role in increasing toughness. Compared to conventional brittle ceramic materials, Ti_3SiC_2 has a layered structure (kink band) that can absorb different deformation mechanisms when faced with tension (their structures have a strong metal bond and a partially weak covalent bond at the same time). These mechanisms cause to limitation of damage, so the homogeneous distribution of stress reduces matrix sensitivity to stress concentrations [28, 37-40].

After the three-point bending test, the fractured surfaces were examined by SEM to get information about the
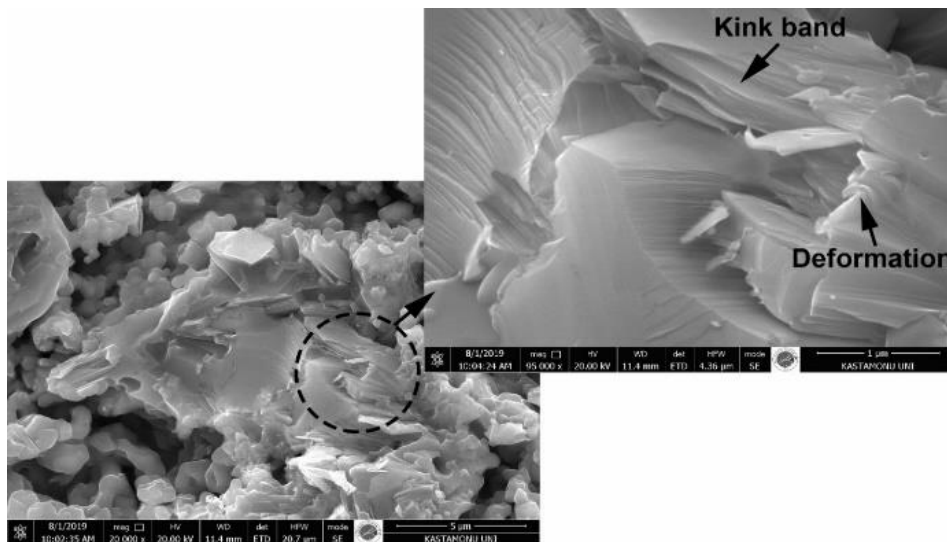
Fig. 13. SEM photographs of the broken surface of the sintered sample at 1150 °C
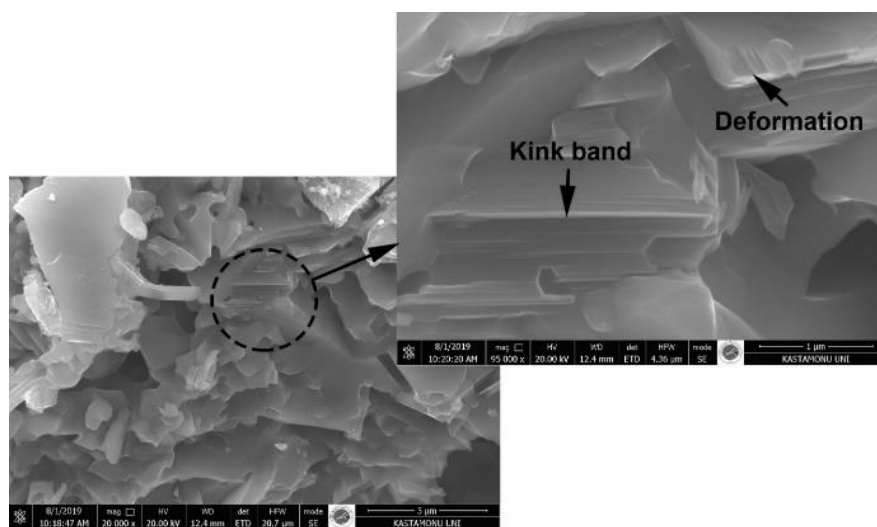
Fig. 14. SEM photographs of the broken surface of the sintered sample at 1300 °C
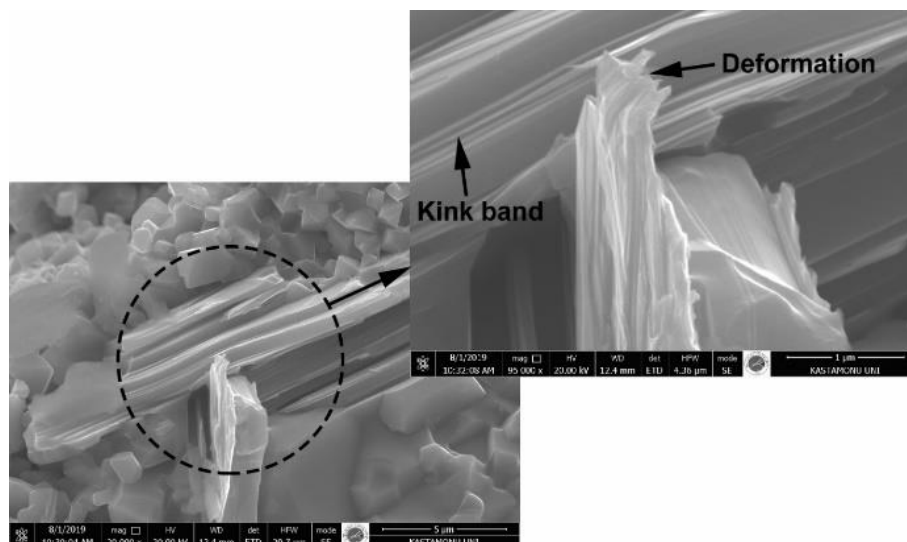
Fig. 15. SEM photographs of the broken surface of the sintered sample at 1450 °C

4. CONCLUSIONS

In this study, which aims to investigate the production and characterization of MAX phase materials by powder metallurgy method, the following information, findings and results have been reached.

1) Ti₃SiC₂-CNF composite materials have been successfully produced using powder metallurgy method. Sintering temperature was preferred as the production parameter and the effects of this sintering temperature on some properties were determined.

2) According to XRD analysis, SiC, TiC, C, Ti₃SiC₂, Ti₅Si₃ and TiSi₂ phases were detected at all three sintering temperatures (1150 °C, 1300 °C and 1450 °C). It was determined that the intensity of Ti₃SiC₂ MAX phase increased even more with increasing sintering temperature.

3) With the increase of sintering temperature, both the experimental and relative densities of the samples have increased significantly. Microhardness values have changed considerably with increasing sintering temperature. As the sintering temperature increased, the TRS values of the samples increased.

DECLARATION OF ETHICAL STANDARDS

The author(s) of this article declare that the materials and methods used in this study do not require ethical committee permission and/or legal-special permission.

REFERENCES

[1]   Barsoum M. W., "The M_{N+1}AX_N phases: A new class of solids: Thermodynamically stable nanolaminates", *Progress in Solid State Chemistry*, 28: 201-281, (2000).

[2]   Sun Z. M., Hashimoto H., Zhang Z. F., Yang S. L., Tada S., "Synthesis and characterization of a metallic ceramic material–Ti₃SiC₂", *Materials Transactions*, 47: 170-174, (2006).

[3]   Amini S., Ni C., Barsoum M. W., "Processing microstructural characterization and mechanical properties of a Ti₂AlC/Nanocrystalline Mg-matrix composite", *Composites Science and Technology*, 69: 414-420, (2009).

[4]   Palmquist J. P., Li S., Persson P Å., Emmerlich J., Wilhelmsson O., Högberg H., Katsnelson M.I., Johansson B., Ahuja R., Eriksson O., Hultman L., Jansson U., "M_{n+1}AX_n phases in the Ti−Si−C system studied by thin-film synthesis and ab initio calculations", *Physical Review B*, 70: 165401, (2004).

[5]   Lin Z., Zhuo M., Zhou Y., Li M., Wang J., "Microstructures and theoretical bulk modulus of layered ternary tantalum aluminium carbides", *Journal of the American Ceramic Society*, 89: 3765-3769, (2006).

[6]   Bouhemadou A., "Structural, electronic and elastic properties of MAX phases M₂GaN (M= Ti, V and Cr)", *Solid State Sciences*, 11: 1875-1881, (2009).

[7]   Music D., Sun Z., Schneider J. M., "Electronic structure of Sc₂AC (A= Al, Ga, In, Tl)", *Solid State Communications*, 133: 381-383, (2005).

[8]   Music D., Sun Z., Voevodin A. A., Schneider J. M., "Electronic structure and shearing in nanolaminated ternary carbides", *Solid State Communications*, 139: 139-143, (2006).

[9]   Bouhemadou A., Khenata R., Chegaar M., "Structural and elastic properties of Zr₂AlX and Ti₂AlX (X= C and N) under pressure effect", *The European Physical Journal B*, 56: 209-215, (2007).

[10]   Bouhemadou A., "Prediction study of structural and elastic properties under pressure effect of M₂SnC (M= Ti, Zr, Nb, Hf)", *Physica B: Condensed Matter*, 403: 2707-2713, (2008).

[11]   Sun Z. M., Yang S., Hashimoto H., Tada S., Abe T., "Synthesis and consolidation of ternary compound Ti₃SiC₂ from green compact of mixed powders", *Materials Transactions*, 45: 373-375, (2004).

[12]   Sun Z. M., "Progress in research and development on MAX phases: a family of layered ternary compounds", *International Materials Reviews*, 56: 143-166, (2011).

[13] Chang F., Li C., Yang J., Tang H., Xue M., "Synthesis of a new graphene-like transition metal carbide by de-intercalating Ti_3AlC_2", *Materials Letters*, 109: 295-298, (2013).

[14] Kero I., Tegman R., Antti M. L., "Phase reactions associated with the formation of Ti_3SiC_2 from TiC/Si powders", *Ceramics International*, 37: 2615-2619, (2011).

[15] Hug G., Eklund P., Orchowski A., "Orientation dependence of electron energy loss spectra and dielectric functions of Ti_3SiC_2 and Ti_3AlC_2", *Ultramicroscopy*, 110: 1054-1058, (2010).

[16] Li D., Liang Y., Liu X., Zhou Y., "Corrosion behavior of Ti_3AlC_2 in NaOH and H_2SO_4", *Journal of the European Ceramic Society*, 30: 3227-3234, (2010).

[17] Thomas T., Bowen C. R., "Thermodynamic predictions for the manufacture of Ti_2AlC MAX-phase ceramic by combustion synthesis", *Journal of Alloys and Compounds*, 602: 72-77, (2014).

[18] Oh H. C., Lee S. H., Choi S. C., "The reaction mechanism for the low temperature synthesis of Cr_2AlC under electronic field", *Journal of Alloys and Compounds*, 587: 296-302, (2014).

[19] Li S., Li H., Zhou Y., Zhai H., "Mechanism for abnormal thermal shock behavior of Cr_2AlC", *Journal of the European Ceramic Society*, 34: 1083-1088, (2014).

[20] Abdulkadhim A., To Baben M., Schnabe V., Hans M., Thieme N., Polzer C., Polcik P., Schneider J. M., "Crystallization kinetics of V_2AlC", *Thin Solid Films*, 520: 1930-1933, (2012).

[21] Chunfeng H., Yoshio S., Salvatore G., Toshiyuki N., Shuqi G., Hidehiko T., "Shell-like nanolayered Nb_4AlC_3 ceramic with high strength and toughness", *Scripta Materialia*, 64: 765-768, (2011).

[22] Ghebouli M. A., Ghebouli B., Bouhemadou A., Fatmi M., "Theoretical study of the structural, elastic, electronic and thermal properties of the MAX phase Nb_2SiC", *Solid State Communications*, 151: 382-387, (2011).

[23] Ortiz A. L., Cumbrera F. L., Sánchez-Bajo F., Guiberteau F., Xu H., Padture N. P., "Quantitative phase-composition analysis of liquid-phase-sintered silicon carbide using the rietveld method", *Journal of the American Ceramic Society*, 83: 2282-2286, (2000).

[24] Singh A., Bakshi S. R., Virzi D. A., Keshri A. K., Agarwal A., Harimkar S. P., "In-situ synthesis of $TiC/SiC/Ti_3SiC_2$ composite coatings by spark plasma sintering", *Surface and Coatings Technology*, 205: 3840-3846, (2011).

[25] Calado L. D., Padilha G. S., Osório W. R., Bortolozo A. D., "Designing sintering time for a TiSiC compound: a microwave and conventional comparison", *The International Journal of Advanced Manufacturing Technology*, 104(1-4): 1561-1570, (2019).

[26] Bale C. W., Chartrand P., Degterov S. A., Eriksson G., Hack K., Ben Mahfoud R., Melançon J., Pelton A.D., Petersen S., "FactSage thermochemical software and databases", *Calphad*, 26: 189-228, (2002).

[27] Ding H., Chu W., Wang Q., Miao W., Wang H., Liu Q., Glandut N., Li C., "The in-situ synthesis of TiC in Cu melts based on Ti–C–Si system and its mechanism", *Materials & Design*, 182: 108007, (2019).

[28] Yaghobizadeh O., Sedghi A., Baharvandi H. R., "Mechanical properties and microstructure of the CC-SiC, $CC-SiC-Ti_3SiC_2$ and $CC-SiC-Ti_3Si(Al)C_2$ composites", *Materials Science and Engineering: A*, 731: 446-453, (2018).

[29] Wakelkamp W. J. J., Van Loo F. J. J., Metselaar R., "Phase relations in the Ti-Si-C system", *Journal of the European Ceramic Society*, 8: 135-139, (1991).

[30] Min K. H., Lee B. H., Chang S. Y., Do Kim Y., "Mechanical properties of sintered 7xxx series Al/SiC_p composites", *Materials Letters*, 61: 2544-2546, (2007).

[31] Islak S., Kır D., Buytoz S., "Effect of sintering temperature on electrical and microstructure properties of hot pressed Cu-TiC composites", *Science of Sintering*, 46: 15-21, (2014).

[32] Darabi M., Rajabi M., Junipour B., Noghani M. T., "The effect of sintering temperature on Cu-CNTs nano composites properties Produced by PM Method", *Science of Sintering*, 50: 477-486, (2018).

[33] Liu Y., Chen J., Zhou Y., "Effect of Ti_5Si_3 on wear properties of $Ti_3Si(Al)C_2$", *Journal of the European Ceramic Society*, 29: 3379-3385, (2009).

[34] Magnus C., Cooper D., Ma L., Rainforth W. M., "Microstructures and intrinsic lubricity of in situ Ti_3SiC_2–$TiSi_2$–TiC MAX phase composite fabricated by reactive spark plasma sintering (SPS)", *Wear*, 448-449: 203169, (2020).

[35] Islak S., Çelik H., "Effect of sintering temperature and boron carbide content on the wear behavior of hot pressed diamond cutting segments", *Science of Sintering*, 47: 131-143, (2015)

[36] Jiang Y., Liu X., Gao H., He, Y., "Reactively Synthesized Porous Ti_3SiC_2 Compound and its Mechanical Properties with Different Apertures", *Crystals*, 10(2): 82, (2020).

[37] Curtin W. A., "Theory of mechanical properties of ceramic-matrix composites", *Journal of the American Ceramic Society*, 74: 2837-2845, (1991).

[38] Pompidou S., Lamon J., "Analysis of crack deviation in ceramic matrix composites and multilayers based on the Cook and Gordon mechanism", *Composites Science and Technology*, 67: 2052-2060, (2007).

[39] Ly H. Q., Taylor R., Day R. J., Heatley F., "Conversion of polycarbosilane (PCS) to SiC-based ceramic Part 1 Characterisation of PCS and curing products", *Journal of Materials Science*, 36: 4037-4043, (2001).

[40] Wang Z., Jiang Y., Liu X., He Y., "Pore structure of reactively synthesized nanolaminate Ti_3SiC_2 alloyed with Al", *Ceramics International*, 46(1): 576-583, (2020)